
Prediction intervals for overdispersed binomial endpoints and their application to historical control data

Max Menssen^{1*}, Jonathan Rathjens²

*: Corresponding author

1: Department of Biostatistics, Leibniz University Hannover

2: Early Development Statistics, Chrestos Concept GmbH & Co. KG, Essen

Abstract

In toxicology, the validation of the concurrent control by historical control data (HCD) has become requirements. This validation is usually done by historical control limits (HCL) which in practice are often graphically displayed in a Sheward control chart like manner. In many applications, HCL are applied to dichotomous data, e.g. the number of rats with a tumor vs. the number of rats without a tumor (carcinogenicity studies) or the number of cells with a micronucleus out of a total number of cells. Dichotomous HCD may be overdispersed and can be heavily right- (or left-) skewed, which is usually not taken into account in the practical applications of HCL.

To overcome this problem, four different prediction intervals (two frequentist, two Bayesian), that can be applied to such data, are proposed. Comprehensive Monte-Carlo simulations assessing the coverage probabilities of seven different methods for HCL calculation reveal, that frequentist bootstrap calibrated prediction intervals control the type-1-error best. Heuristics traditionally used in control charts (e.g. the limits in Sheward np-charts or the mean ± 2 SD) as well as the historical range fail to control a pre-specified coverage probability.

The application of HCL is demonstrated based on a real life data set containing historical controls from long-term carcinogenicity studies run on behalf of the U.S. National Toxicology Program. The proposed frequentist prediction intervals are publicly available from the R package `predint`, whereas R code for the computation of the Bayesian prediction intervals is provided via GitHub.

Keywords: Bootstrap-calibration, micro-nucleus-test, long-term carcinogenicity studies, OECD test guideline, Sheward control chart, Bayesian hierarchical modeling

1 Introduction

For several toxicological or pre-clinical study types it is mandatory to store and report the outcome of the negative and sometimes also positive control groups of the experiments conducted before the current study (see e.g. OECD guidelines 471, 487, 489 or EFSA 2024).

In the context of the current study, such historical control data (HCD) can be applied in several ways: One possible application is the inclusion of HCD into the test procedure in order to enhance the power of the current test or to reduce individuals in the concurrent control group (Tarone 1982a, Tarone 1982b, Ryan 1993, Kitsche 2012, Bonapersona et al. 2021, Gurjanov et al. 2021, Gurjanov et al. 2024a, Gurjanov et al. 2024ab). Another possible application is the validation of the concurrent negative (or positive) control group by so called historical control limits (HCL) that aim to define the central x % (usually 95 %) of the underlying distribution of the HCD. Consequently, HCL aim to cover the observation(s) of a current control group with the predefined probability (Kluxen et al. 2021, Dertinger et al. 2023, Menssen 2023). This approach is seen as a quality check for the current control group(s) and it is interpreted as a warning signal, if the current control is not covered by the HCL (Vandenberg et al. 2020): Either as a warning for a false-positive result of the current study (if the concurrent control falls below the lower HCL) or as a warning for a false-negative result (if the concurrent control falls above the upper HCL).

Despite the fact, that the HCL based validation of a current control is required by several test guidelines (OECD 471, OECD 473, OECD 487, OECD 490), most guidelines fail to provide reproducible methodology on how to compute HCL. Hence, many heuristics such as the historical range or the mean \pm 2 SD are used for the practical calculation of HCL, but all heuristics have severe theoretical drawbacks. For a discussion of this topic see Menssen 2023. However, this problem can be overcome by the application of prediction intervals which based on historical observations (the HCD) directly aim for the prediction of one (or more) values of the same data generating process (the current control group). Hence several authors recommend the use of prediction intervals for the application of HCL (EFSA 2024, Menssen and Schaarschmidt 2019, Menssen and Schaarschmidt 2022, Menssen 2023, Kluxen et al. 2021, Dertinger et al. 2023).

In toxicology several study types assess dichotomous endpoints: e.g. Carcinogenicity studies (rats with vs. rats without a tumor), the micro nucleus test (cells with vs. cells without a micronucleus) or the recently developed liquid microplate fluctuation Ames MPFTM test following Spiliotopoulos et al. 2024 (numbers of wells with vs. number of wells without a color change). It seems natural to model such data based on the binomial distribution.

But, the clustered nature of the HCD (a certain number of experimental units belong to a certain control group) gives rise for systematic between-study variation. With other words, in many cases the variability of the data exceeds the variance that can be modeled by the simple binomial distribution. This effect is called overdispersion (or extra-binomial variation) and can be commonly found in real life HCD (see supplementary materials section 4) meaning that, possible overdispersion has to be accounted for in the calculation of historical control limits (Menssen and Schaarschmidt 2019, Menssen et al. 2024). Hence, the aim of this paper is to provide reproducible methodology for the calculation of prediction intervals for overdispersed binomial endpoints, that satisfactorily cover the number of affected experimental units in a current control group with the desired probability (e.g. 95 %). The paper is organized as follows: The next section provides an overview about the modeling of overdispersed binomial endpoints. Section 3 provides an overview about several heuristical methods for the calculation of HCL. Furthermore this section proposes four different methods for the calculation of prediction intervals (two frequentist, two Bayesian). Section 4 reviews the properties of two real life HC data bases, that serve as an inspiration for Monte-Carlo simulations regarding the coverage probabilities of the proposed methodology (section 5). The application of the proposed methods is demonstrated in section 6. The manuscript ends with a discussion (section 7) and some conclusions (section 8).

2 Models for overdispersed binomial data

Routinely, dichotomous data is modeled based on the binomial distribution, such that

$$Y \sim \text{Bin}(n, \pi) \tag{1}$$

$$E(Y) = n\pi$$

$$\text{var}(Y) = n\pi(1 - \pi)$$

with π as the binomial proportion, and Y number of events out of n experimental units.

However, this approach ignores the clustered structure of the historical control data that is usually comprised of $h = 1, \dots, H$ historical control groups of which each contains $1, \dots, n_h$ experimental units (e.g. rats). This clustering gives rise to possible between-study

overdispersion, meaning that the variability of the data exceeds the variability of a simple binomial random variable. This effect can be caused by positive correlations between the experimental units within each cluster (Demetrio et al. 2014, McCullagh and Nelder 1989). For example, in the context of two-year carcinogenicity studies it is likely, that rats *within* each control group descent from the same batch of animals which are operated by the same lab personnel, but batches, personnel and other factors are likely to change *between* different studies. If the tumor rate of some batches is systematically above (or below) average, the number of rats per batch or (historical) control group are no longer independent observations of the same simple binomial distribution as given in eq. 1, because they are positively correlated.

One possible way to model overdispersed binomial data is the beta-binomial distribution in which the binomial proportion for each cluster are derived from a beta distribution

$$\pi_h \sim \text{beta}(a, b)$$

and the random variable within each cluster is binomial

$$Y_h \sim \text{Bin}(n_h, \pi_h).$$

In this setting $E(\pi_h) = \pi = a/(a + b)$ and $E(Y_h) = n_h\pi$. The variance is

$$\text{var}(Y_h) = n_h\pi(1 - \pi)[1 + (n_h - 1)\rho]. \quad (2)$$

In this parametrisation $\rho = 1/(1 + a + b)$ describes the intra-class correlation coefficient (Lui et al. 2000). Please note, that the parameters of the beta distribution are restricted to be $a > 0$ and $b > 0$. Hence also the intra-class correlation is restricted to be $\rho > 0$.

Another possibility to model between-study overdispersion is the quasi-binomial approach in which the dispersion parameter ϕ constantly inflates the variance

$$\text{var}(Y_h) = n_h\pi(1 - \pi)\phi. \quad (3)$$

Note, that in the case in which the number of experimental unis within each control group becomes equal ($n_h = n_{h'} = n$) also the part of the beta-binomial variance that controls the magnitude of overdispersion per control group ($[1 + (n_h - 1)\rho]$ in eq. 2) becomes a constant. Consequently, both models are not in contradiction in this special case (Menssen and Schaarschmidt 2019).

3 Historical control limits for overdispersed binomial data

The calculation of the historical control limits $[l, u]$ given below is based on the observed number of experimental units with an event y_h out of a total number of experimental units n_h (e.g. rats with a tumor out of a total number of rats). All historical control limits (HCL) are aimed to cover a further number of experimental units with an event y^* out of a further total number of experimental units n^* with coverage probability

$$P(l \leq y^* \leq u) = 1 - \alpha. \quad (4)$$

This means that the historical HCL are aimed to approximate the central $100(1 - \alpha)\%$ of the underlying distribution of y^* . But, overdispersed binomial data can become highly right- or left-skewed, meaning that the skeweness increases the more π approaches its boundaries (0 or 1) and/or the lower the sample size n_h gets (see fig. 1 and 2 of the supplementary material).

Hence, it is crucial, that the desired HCL account for equal tail probabilities (Hoffmann 2003) in a way that

$$P(l \leq y^*) = P(y^* \leq u) = 1 - \alpha/2. \quad (5)$$

In this case, the HCL are aimed to converge against the true $\alpha/2$ and $1 - \alpha/2$ quantiles of the true underlying distribution of y^* and hence, control its center (Francq et al. 2019, Menssen 2023).

3.1 Heuristical historical control limits

Although several authors, dissuade from its use (Greim et al. 2003, Kluxen et al. 2021, EFSA 2024, Menssen 2023), HCL based on the historical range are frequently applied in daily toxicological routine. Since such HCL are given by

$$\left[l = \min(y_h), u = \max(y_h) \right] \quad (6)$$

they are aimed to cover *all* observations of the underlying distribution and hence, do not aim for a proper approximation of its central $100(1 - \alpha)\%$.

Another popular method for the calculation of control limits for dichotomous data are the limits used in Sheward np-charts

$$[l, u] = n^* \bar{\pi} \pm k \sqrt{n^* \bar{\pi} (1 - \bar{\pi})} \quad (7)$$

with $\bar{\pi} = \frac{\sum_h y_h}{\sum_h n_h}$. In practical applications k is usually set to 2 or 3 in order to approximate the central 95.4 % or 99.7 % of the underlying distribution (Montgomery 2019). This HCL are strictly based on the assumption that the observations are independent realizations of the same binomial distribution which can be adequately approximated by a normal distribution with mean $n^* \bar{\pi}$ and variance $n^* \bar{\pi} (1 - \bar{\pi})$. Hence, the Sheward np-chart presumes that the law of large numbers is applicable, but neither allows for overdispersion, nor ensures for equal tail probabilities.

HCL that are based on the mean $\pm k$ standard deviations are given by

$$[l, u] = \bar{y} \pm kSD \quad (8)$$

with $\bar{y} = \frac{\sum_h y_h}{H}$ and $SD = \sqrt{\frac{\sum_h (\bar{y} - y_h)^2}{H-1}}$. This type of HCL is based on a simple normal approximation that lacks an explicit assumption about the mean-variance relationship and hence heuristically allows for overdispersion (Menssen et al. 2024). However, it is also based on the assumption that all observations have the same variance, which, for dichotomous data, is only the case, if all control groups (historical, current or future) have the same sample size $n_h = n^* \quad \forall h = 1, \dots, H$ (see eq. 2 and 3). Hence, the application of HCL that are computed by the mean $\pm k$ standard deviations to dichotomous HCD with different sample sizes should strictly be avoided (see section 2 of the supplementary material).

3.2 Bootstrap calibrated prediction intervals

Similarly to the prediction intervals for overdispersed count data of Menssen et al. 2024, the two frequentist prediction intervals below are based on the assumption that

$$\frac{\hat{y}^* - Y^*}{\sqrt{\widehat{var}(\hat{y}^* - Y^*)}} = \frac{\hat{y}^* - Y^*}{\sqrt{\widehat{var}(\hat{y}^*) + \widehat{var}(Y^*)}} = \frac{n^* \hat{\pi} - Y^*}{\sqrt{\widehat{var}(n^* \hat{\pi}) + \widehat{var}(Y^*)}}$$

is approximately normal. In this notation, \hat{y}^* is the expected further observation, $\hat{\pi}$ is the estimate for the binomial proportion estimated from the HCD, n^* is the sample size for the predicted observation and the standard error of the prediction is given by

$$\widehat{se}(\hat{y}^* - Y^*) = \sqrt{\widehat{var}(\hat{y}^*) + \widehat{var}(Y^*)} = \sqrt{\widehat{var}(n^* \hat{\pi}) + \widehat{var}(Y^*)}.$$

According to Nelson 1982, the corresponding prediction interval for binomial observations is given as

$$[l, u] = n^* \hat{\pi} \pm z_{1-\alpha/2} \sqrt{\frac{n^{*2} \hat{\pi}(1 - \hat{\pi})}{n} + n^* \hat{\pi}(1 - \hat{\pi})}. \quad (9)$$

This interval is explicitly based on the assumption that the HCD is an unstructured sample of n experimental units and hence does not allow for overdispersion. Furthermore, it is a symmetrical interval that is based on normal approximation and consequently does not account for equal tail probabilities. Hence the prediction interval given in eq. 9 has to be adapted in a way, that allows its application to clustered HCD which possibly exhibits between-study overdispersion and a skewed distribution. This is done in two steps. Firstly, the asymptotic prediction intervals of Nelson is adapted to overdispersion. In a second step these intervals are adapted to possible skeweness using bootstrap calibration.

If between-study overdispersion is modeled based on the quasi-binomial assumption the prediction standard error becomes $\widehat{se}(\hat{y}^* - Y^*) = \sqrt{\frac{\hat{\phi} n^{*2} \hat{\pi}(1 - \hat{\pi})}{\sum_h n_h} + \hat{\phi} n^* \hat{\pi}(1 - \hat{\pi})}$ with $\hat{\phi} > 1$ as an estimate for the between-study overdispersion. According to Menssen and Schaarschmidt 2019, the corresponding prediction interval is given by

$$[l, u] = n^* \hat{\pi} \pm z_{1-\alpha/2} \sqrt{\frac{\hat{\phi} n^{*2} \hat{\pi}(1 - \hat{\pi})}{\sum_h n_h} + \hat{\phi} n^* \hat{\pi}(1 - \hat{\pi})} \quad (10)$$

If between-study overdispersion is modeled based on the beta-binomial distribution, the prediction standard error becomes

$$\widehat{se}(\hat{y}^* - Y^*) = \sqrt{\left[\frac{n^{*2} \hat{\pi}(1 - \hat{\pi})}{\sum_h n_h} + \frac{\sum_h n_h - 1}{\sum_h n_h} n^{*2} \hat{\pi}(1 - \hat{\pi}) \hat{\rho} \right] + n^* \hat{\pi}(1 - \hat{\pi}) [1 + (n^* - 1) \hat{\rho}]}$$

with $\hat{\rho}$ as an estimate for the intra-class correlation coefficient. The corresponding prediction interval is given by

$$[l, u] = n^* \hat{\pi} \pm z_{1-\alpha/2} \sqrt{\left[\frac{n^{*2} \hat{\pi}(1 - \hat{\pi})}{\sum_h n_h} + \frac{\sum_h n_h - 1}{\sum_h n_h} n^{*2} \hat{\pi}(1 - \hat{\pi}) \hat{\rho} \right] + n^* \hat{\pi}(1 - \hat{\pi}) [1 + (n^* - 1) \hat{\rho}]}. \quad (11)$$

As mentioned above, overdispersed binomial data can be heavily right- or left-skewed, but the prediction intervals in eq. 10 and 11 are still symmetrical intervals. To overcome this problem, a bootstrap calibration algorithm (see box below), that individually calibrates both interval borders was applied.

Bootstrap calibration of the proposed prediction intervals

1. Based on the historical data \mathbf{y} find estimates for the model parameters $\hat{\boldsymbol{\theta}}$, with $\hat{\boldsymbol{\theta}} = (\hat{\pi}, \hat{\phi})$ in the quasi-binomial case and $\hat{\boldsymbol{\theta}} = (\hat{\pi}, \hat{\rho})$ in the beta-binomial case
2. Based on $\hat{\boldsymbol{\theta}}$, sample B parametric bootstrap samples \mathbf{y}_b following the same experimental design as the historical data (for sampling algorithms see section 3 of the supplementary material)
3. Draw B further bootstrap samples y_b^* following the same experimental design as the current observations
4. Fit the initial model to \mathbf{y}_b in order to obtain $\hat{\boldsymbol{\theta}}_b$
5. Based on $\hat{\boldsymbol{\theta}}_b$, calculate $\widehat{var}_b(n^*\hat{\pi})$ and $\widehat{var}_b(Y^*)$
6. Calculate lower prediction borders $l_b = n^*\hat{\pi}_b - q_l \sqrt{\widehat{var}_b(n^*\hat{\pi}) + \widehat{var}_b(Y^*)}$, such that all l_b depend on the same value for q_l .
7. Calculate the bootstrapped coverage probability $\hat{\psi}_l = \sum_b I_b$ with $I_b = 1$ if $l_b \leq y_b^*$ and $I_b = 0$ if $y_b^* < l_b$
8. Alternate q_l until $\hat{\psi}_l \in (1 - \frac{\alpha}{2}) \pm t$ with t as a predefined tolerance around $1 - \frac{\alpha}{2}$
9. Repeat steps 5-7 for the upper prediction border with $\hat{\psi}_u = \sum_b I_b$ with $I_b = 1$ if $y_b^* \leq u_b$ and $I_b = 0$ if $u_b < y_b^*$
10. Use the corresponding coefficients q_l^{calib} and q_u^{calib} for interval calculation

$$\begin{aligned} l &= n^*\hat{\pi} - q_l^{calib} \sqrt{\widehat{var}(n^*\hat{\pi}) + \widehat{var}(Y^*)}, \\ u &= n^*\hat{\pi} + q_u^{calib} \sqrt{\widehat{var}(n^*\hat{\pi}) + \widehat{var}(Y^*)} \end{aligned}$$

A similar algorithm was used by Menssen et al. 2024 in order to calibrate prediction intervals for overdispersed count data. Both algorithms are modified versions of the bootstrap calibration procedure of Menssen and Schaarschmidt 2022. The only difference to Menssen and Schaarschmidt 2022 is, that both interval limits are calibrated individually, but the search for q_l^{calib} and q_u^{calib} depends on the same bisection procedure using a tolerance $t = 0.001$.

The bootstrap calibrated quasi-binomial prediction interval is given by

$$\begin{aligned} l &= n^* \hat{\pi} - q_l^{calib} \sqrt{\frac{\hat{\phi} n^{*2} \hat{\pi} (1 - \hat{\pi})}{\sum_h n_h} + \hat{\phi} n^* \hat{\pi} (1 - \hat{\pi})} \\ u &= n^* \hat{\pi} + q_u^{calib} \sqrt{\frac{\hat{\phi} n^{*2} \hat{\pi} (1 - \hat{\pi})}{\sum_h n_h} + \hat{\phi} n^* \hat{\pi} (1 - \hat{\pi})}. \end{aligned}$$

Similarly, the bootstrap calibration of the beta-binomial prediction interval results in

$$\begin{aligned} l &= n^* \hat{\pi} - q_l^{calib} \sqrt{n^* \hat{\pi} (1 - \hat{\pi}) [1 + (n^* - 1) \hat{\rho}] + \left[\frac{n^{*2} \hat{\pi} (1 - \hat{\pi})}{\sum_h n_h} + \frac{\sum_h n_h - 1}{\sum_h n_h} n^{*2} \hat{\pi} (1 - \hat{\pi}) \hat{\rho} \right]} \\ u &= n^* \hat{\pi} + q_u^{calib} \sqrt{n^* \hat{\pi} (1 - \hat{\pi}) [1 + (n^* - 1) \hat{\rho}] + \left[\frac{n^{*2} \hat{\pi} (1 - \hat{\pi})}{\sum_h n_h} + \frac{\sum_h n_h - 1}{\sum_h n_h} n^{*2} \hat{\pi} (1 - \hat{\pi}) \hat{\rho} \right]}. \end{aligned}$$

3.3 Bayesian modeling

Bayesian approaches provide an alternative estimation of prediction intervals (Hamada et al. 2004). Future observations as well as all model parameters are interpreted as random variables depending on each other. Thus, a posterior distribution of a future observation can be derived immediately within the parameter estimation process.

As above, a situation with historical experiments $h = 1, \dots, H$ is considered, but individual observations $i = 1, \dots, I$ per experiment are possible. Let n_{hi} be the total numbers of experimental units and $Y_{hi} \in \{0, 1, \dots, n_{hi}\}$ the numbers of successes among them. As before, the data are modeled on experiment level by aggregation:

$$n_h = \sum_{i=1}^I n_{hi}$$

$$Y_h = \sum_{i=1}^I Y_{hi}$$

Furthermore, for Bayesian modeling the total number of experimental units is assumed to be constant over all clusters (historical and current control groups):

$$n_{hi} =: n' \Rightarrow n_h = n^* = In =: n \quad \forall h.$$

3.3.1 Hierarchical modeling

If we assume the binomial model

$$Y_{hi} \sim \text{Bin}(n_{hi}, \pi_h) = \text{Bin}(n', \pi_h)$$

for individual values, it follows

$$Y_h \sim \text{Bin}(n, \pi_h)$$

per historical control group.

This is the same situation as above, and again a Beta-binomial model is applied to represent the between-experiment-overdispersion. In a Bayesian interpretation, the experiments' parameters π_h are assumed to follow a Beta distribution, as a second level in a hierarchy (Howley and Gibbert 2003).

A Beta prior in mean-precision-parametrization (Beta proportion distribution) is applied (Stan development Team 2024a):

$$\pi_h \sim \text{Be}(\mu, \kappa) \quad \forall h$$

with a non-informative prior for the location hyperparameter $\mu \in (0, 1)$. A weakly informative gamma prior $\kappa \sim \text{Ga}(a, b)$ should be applied to represent a realistic domain of the precision hyperparameter $\kappa > 0$ and, thus, to obtain a stable estimation.

The parameters' posterior distributions, given the data, i.e. symbolically

$$\begin{aligned} p(\pi_1, \dots, \pi_H, \mu, \kappa \mid Y_1, \dots, Y_H) &\propto p(Y_1, \dots, Y_H \mid \pi_1, \dots, \pi_H) p(\pi_1, \dots, \pi_H \mid \mu, \kappa) p(\mu, \kappa) = \\ &p(\mu, \kappa) \prod_{h=1}^H p(\pi_h \mid \mu, \kappa) p(Y_h \mid \pi_h) \end{aligned}$$

are estimated by Markov-chain-Monte-Carlo (MCMC) sampling.

A posterior predictive distribution of a future observation y^* is obtained by random sampling per MCMC iteration $c = 1, \dots, C$: For every MCMC sample $(\hat{\mu}_c, \hat{\kappa}_c)$ of μ and κ , a prediction

$$\hat{\pi}_c^* \sim \text{Be}(\hat{\mu}_c, \hat{\kappa}_c)$$

of the future experiment's success proportion is drawn, and in turn a predicted future observation is sampled as

$$y_c^* \sim \text{Bin}(n, \hat{\pi}_c^*).$$

A pointwise prediction interval for one future observation y^* is then obtained using empirical quantiles of $\{y_1^*, \dots, y_C^*\}$ such that

$$[l, u] = [q_{\alpha/2}(\{y_1^*, \dots, y_C^*\}), q_{1-\alpha/2}(\{y_1^*, \dots, y_C^*\})]$$

in the two-sided case.

3.3.2 Bayesian generalized linear mixed model

A concept closely related to the above Beta-binomial model is a generalized linear mixed model (GLMM), where Bernoulli distributed random variables Z_{h1}, \dots, Z_{hn} with $\sum_{k=1}^n Z_{hk} = Y_h$ are considered (Fong et al. 2010). The success proportion $\pi_h = E(Z_{hk})$ is linked to a linear predictor

$$\eta_h = \ln \frac{\pi_h}{1 - \pi_h} \in (-\infty, +\infty),$$

which is comprised of a fixed general intercept ν and random intercepts β_h per experiment:

$$\eta_h = \nu + \beta_h, \quad \beta_h \sim N(0, \sigma).$$

With that, the historical experiments are again assumed to have individual success proportions π_h , derived from the same distribution, and the observations are again realizations of the binomial random variable $Y_h \sim \text{Bin}(n, \pi_h)$.

The posterior distributions of $\nu \in (-\infty, +\infty)$ and $\sigma > 0$ are estimated by MCMC sampling using non-informative vague priors. Realizations of the future random variable $Y^* = \sum_{k=1}^n Z_k^*$ are derived similarly to above: For every MCMC sample c , a prediction

$$\hat{\beta}_c^* \sim N(0, \hat{\sigma}_c)$$

of the future experiment's random intercept is drawn, followed by

$$\hat{\eta}_c^* = \hat{\nu}_c + \hat{\beta}_c^*$$

and the future experiment's success proportion

$$\hat{\pi}_c^* = \frac{\exp(\hat{\eta}_c^*)}{\exp(\hat{\eta}_c^*) + 1}$$

are derived, and in turn

$$y_c^* \sim \text{Bin}(n, \hat{\pi}_c^*)$$

is drawn from the latter. Similarly as above, a pointwise two-sided prediction interval for one future observation y^* is given by

$$[l, u] = [q_{\alpha/2}(\{y_1^*, \dots, y_C^*\}), q_{1-\alpha/2}(\{y_1^*, \dots, y_C^*\})].$$

3.4 Computational details and estimation

The proposed frequentist prediction intervals are implemented in the R package **predint** (Menssen 2023). The uncalibrated prediction intervals (eq. 10 and 11) are provided via **qb_pi()** and **bb_pi()**. The bootstrap calibrated prediction intervals (eq. 3.2 and 3.2) are implemented via the functions **quasi_bin_pi()** and **beta_bin_pi()**.

The estimates $\hat{\pi}$ and $\hat{\phi}$ used for the quasi-binomial prediction interval were estimated based on a generalized linear model (**stats::glm()**). The parameter estimates for the beta-binomial distribution $\hat{\pi}$ and $\hat{\rho}$ were estimated following the approach of Lui et al. 2000. Both estimates that define overdispersion were restricted to avoid underdispersion. The quasi-binomial interval was computed with $\hat{\phi} \geq 1.001$. The estimated intra-class correlation used for the beta-binomial interval was restricted to $\hat{\rho} \geq 0.00001$.

The bisection procedure used for bootstrap calibration is implemented in **predint** and provided via the function **bisection()**. This function takes three different lists as input, that contain the bootstrapped expected observations \hat{y}_b^* , the bootstrapped standard errors $\hat{se}(\hat{y}^* - Y^*)_b = \sqrt{\widehat{var}(n^* \hat{\pi})_b + \widehat{var}(Y^*)_b}$ and the bootstrapped further observations y_b^* as input and returns values for q_l and q_u . Hence, this function enables the calculation of bootstrap calibrated prediction intervals in a general way, such that any Wald-type prediction interval can be calibrated, as long as a parametric model can be fit to the data from which parametric bootstrap samples can be sampled.

The Bayesian hierarchical beta-binomial model was applied using the software **stan** via the

R package `rstan` (Stan Development Team 2024). A weakly informative prior $\kappa \sim \text{Ga}(2, 5 \cdot 10^{-5})$ was used, giving the domain of the precision hyperparameter $\kappa > 0$. The Bayesian GLMM was applied using the R function `stan_glmer` from the package `rstanarm` (Goodrich et al. 2024). Functions for the computation of both Bayesian prediction intervals are provided via GitHub https://github.com/MaxMenssen/pi_overdisp_binomial/tree/main.

4 Properties of real life HCD

4.1 HCD from the micro-nucleus test

The occurrence of a micronucleus is an adverse event during cell division, where a small fragment of chromosomes remains outside the new nuclei. Hence, an increase of cells with a micronucleus can be considered as a proxy for the genotoxic properties of a chemical compound (Fenech 2000).

In the in-vitro micro-nucleus test (MNT), cell suspensions are cultivated on a well plate of which some are treated with the test compounds (treatment groups), some are untreated (negative control) and some are treated with a compound with known genotoxic potency to evaluate the test assay's functionality (positive control). At the end of the study, it is examined how many cells (out of a total number of cells) have developed at least one micronucleus.

The setting of the following simulations are inspired by a real life HC data base comprised of negative and positive control groups from about 50 experiments, divided in three parts of about 15 to 20 experiments according to different compounds used for the positive controls. Every control group consists of six wells and 3000 cells were screened each, such that the aggregated number of cells with at least one micronucleus out of a total of 18000 cells was considered.

This HC data base hints at an average proportion of cells with at least one micronucleus of about $\hat{\pi} \approx 0.01$ for negative and about $\hat{\pi} \approx 0.15$ to 0.2 for positive controls. The overdispersion was estimated to range between $\hat{\phi} \approx 10$ and 50 for negative controls and tend to reach several hundreds for positive controls.

4.2 HCD from long-term carcinogenicity studies

Historical control data on different endpoints obtained in long-term carcinogenicity studies (LTC) are provided via the Historical Control Database of the National Toxicology Program (NTP 2024). HCD about the number of B6C3F1 mice per control group that had a hemangioma, the number of mice that showed at least one malignant tumor as well as the number of mice that passed away before the end of the study was analyzed by Menssen and Schaarschmidt 2019 with regard to the binomial proportion $\hat{\pi}$ and the amount of overdispersion $\hat{\phi}$.

For rare events (hemangioma) the reported proportion was relatively low (close to zero) and overdispersion was estimated to be absent in most of the cases. The proportion of animals with malignant tumors ranged between 0.2 and 0.8, whereas the estimated dispersion parameters raised up to roughly four, meaning that the particular data set is four times as variable than possible under simple binomial distribution. The reported mortality rates behaved in a similar fashion.

5 Simulation study

In order to asses the coverage probabilities of the different methods for the calculation of HCL reviewed above, Monte-Carlo simulations were run. In all simulations, the nominal coverage probability was set to $1 - \alpha = 0.95$. The parameter combinations used for the simulation were inspired by the real life data shown above. For all simulations the cluster size was fixed ($n_h = n^* \quad \forall \quad h = 1, \dots, H$) such that the variance-mean relationship of the beta-binomial distribution and the quasi-binomial assumption is not in contradiction to each other.

For each combination of model parameters, $S = 5000$ "historical" data sets were drawn, based on which historical control limits $[l, u]_s$ were calculated. Furthermore, S sets of single "future" observations y_s^* were sampled and the coverage probability of the control intervals

was computed to be

$$\hat{\psi}^{cp} = \frac{\sum_{s=1}^S I_s}{S} \text{ with}$$

$$I_s = 1 \text{ if } y_s^* \in [l, u]_s,$$

$$I_s = 0 \text{ if } y_s^* \notin [l, u]_s.$$

Furthermore, the ability of the different historical control limits to ensure for equal tail probabilities was checked. For this purpose the coverage of the simulated lower borders l_s and upper borders u_s was calculated additionally to the coverage probability for the whole interval. This was done as follows:

$$\hat{\psi}^l = \frac{\sum_{s=1}^S I_s}{S} \text{ with}$$

$$I_s = 1 \text{ if } l_s \leq y_s^*,$$

$$I_s = 0 \text{ if } l_s > y_s^*.$$

and

$$\hat{\psi}^u = \frac{\sum_{s=1}^S I_s}{S} \text{ with} \tag{12}$$

$$I_s = 1 \text{ if } y_s^* \leq u_s,$$

$$I_s = 0 \text{ if } u_s > y_s^*.$$

Each single bootstrap calibrated prediction interval that was calculated in the simulation was based on $B = 10000$ bootstrap samples. Each Bayesian prediction interval was calculated based on $C = 5000$ MCMC samples.

5.1 Coverage probabilities for the MNT-inspired simulation setting

In order to assess the coverage probabilities in a setting that mimics the properties of the real life HCD from the micro-nucleus test, the coverage probabilities for the following 72 combinations of $H = 5, 10, 20, 100$ (the number of historical control groups), $\pi = 0.001, 0.01, 0.1$ (the binomial proportion) and $\phi = 1.001, 3, 5, 10, 50, 500$ (the amount of overdispersion) was assessed for each of the six methods (three heuristics and three prediction intervals). Since cluster size was relatively huge ($n_h = n^* = 18000$) most parameter combinations result in

a relatively symmetrical underlying distribution (except for $\phi = 500$, see supplementary fig. 1).

It is obvious, that the historical range (fig. 1A) covers the future observation y_s^* in all the cases, if the amount of historical control groups is high enough (say above 20). Therefore, the historical range should not be applied for the computation of HCL.

If overdispersion is practically absent ($\phi = 1.001$), the np-chart (fig. 1B) yields coverage probabilities relatively close to the nominal level. With increasing overdispersion (and hence, increasing right-skeweness), the coverage probabilities of the np-chart decrease below 0.2. This demonstrates, that the np-chart should not be applied to toxicological (overdispersed) binomial data.

At first glance, it seems that the HCL computed by the mean ± 2 SD (fig 1C) yield coverage probabilities close to the nominal level of 0.95, if the amount of historical control groups is high enough (at least 20). But, with a decreasing binomial proportion π and/or an increasing amount of overdispersion (ϕ) the right-skeweness of the data increases. Hence, in many cases the lower border almost always covers the future observation (the triangles approach 1) whereas the coverage probability of the upper border (crosses) does not approach the desired 0.975. This behavior demonstrates that HCL computed based on the mean ± 2 SD do not ensure for equal tail probabilities, or in other words: They do not properly cover the central 95 % of the underlying distribution, if this distribution is skewed.

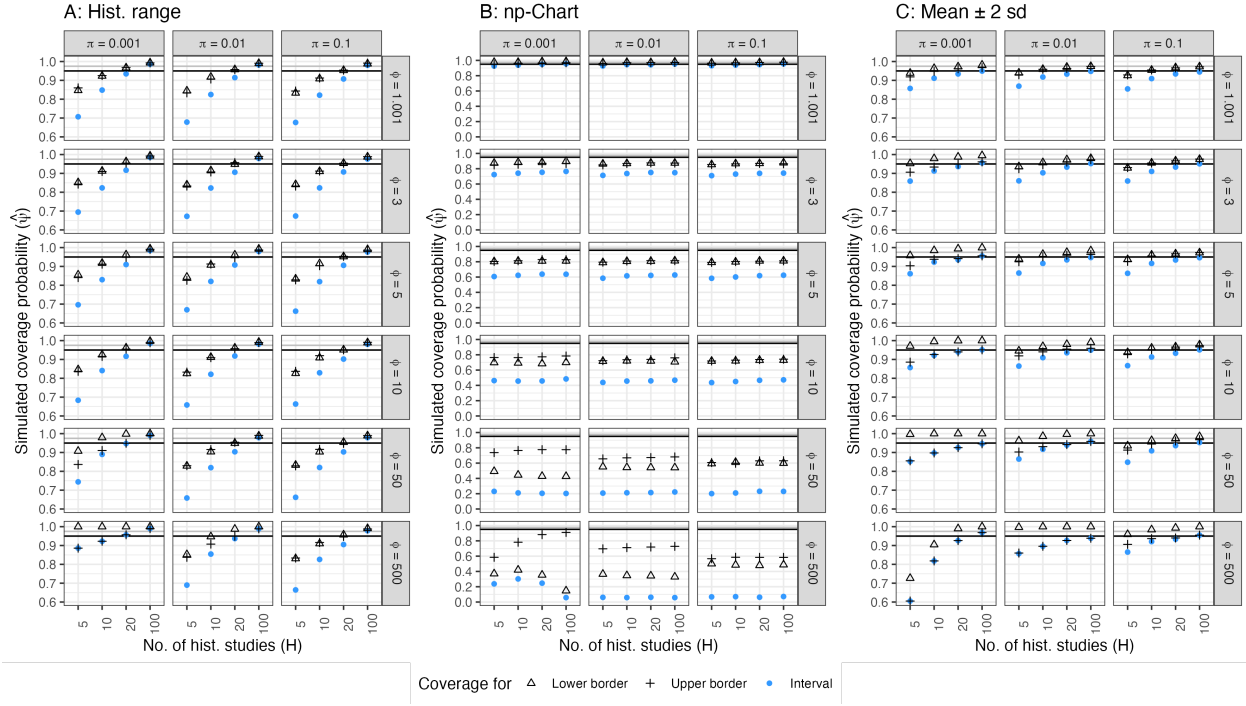


Figure 1: Simulated coverage probabilities of heuristical methods (MNT-setting) **A:** Historical range, **B:** np-chart, **C:** Mean \pm 2 SD, **Black horizontal line:** Nominal coverage probability $\psi^{cp} = 0.95$, **Grey horizontal line:** Nominal coverage probability for the lower and the upper limit, if equal tail probabilities are achieved $\psi^l = \psi^u = 0.975$. Note the different scales of the y-axis of the sub-graphics (0.6-1 for A and C, 0-1 for B).

The coverage probabilities of the three different prediction intervals are depicted in Figure 2. For most of the settings ($\pi \geq 0.01$ and $\phi \in [3, 50]$), the beta-binomial and the quasi-binomial prediction intervals (Fig. 2 A and B) behave in a comparable manner and approach the nominal coverage probability of 0.95, even if only five historical control groups are available. In this settings, the Bayesian prediction interval (Fig. 2C) approaches the nominal coverage probability only for cases where the number of historical control groups is high ($H > 20$), but remains liberal for a lower number of historical control groups.

In the (practical) absence of overdispersion ($\phi = 1.01$), the beta-binomial prediction interval controls the alpha error best, whereas the quasi-binomial prediction interval tends to behave conservatively. But, with an increasing amount of historical control groups, also this interval approaches the nominal coverage probability. Contrary to this, the prediction interval

obtained from Bayesian hierarchical modeling remains conservative in this setting, even for 100 historical studies.

For moderate proportions $\pi \in [0.001, 01]$ and moderate to high overdispersion $\phi \in [3, 50]$ (moderate in the context of $n = 18000$), the quasi- and beta-binomial prediction intervals yield coverage probabilities close to the nominal 0.95, whereas the interval obtained from Bayesian hierarchical modeling approaches the nominal level only for 100 historical studies and remains liberal for a lower amount of historical information.

The right-skewness of the underlying distribution increases with a decreasing binomial proportion and an increasing amount of overdispersion (panels in the lower left of the three sub-graphics). In this case, the sampled data contains many zeros and hence, the computed lower borders always cover the future observation (the triangles approach 1). Hence, the prediction intervals practically aim to yield 97.5 % upper prediction borders. This effect is clearly visible for all three intervals and reflects a core feature of the data rather than being based on model misspecification.

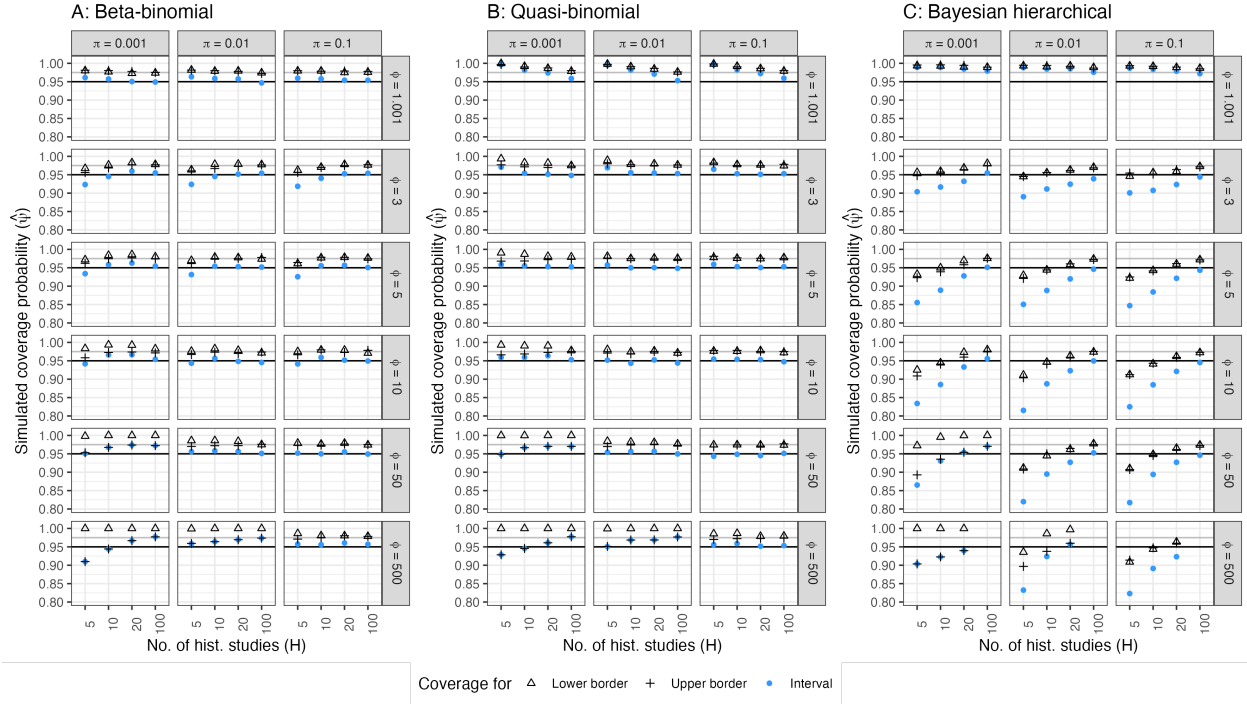


Figure 2: Simulated coverage probabilities of prediction intervals (MNT-setting) **A:** Calibrated beta-binomial prediction interval, **B:** Calibrated quasi-binomial prediction interval, **C:** Prediction interval obtained from a Bayesian hierarchical model, **Black horizontal line:** Nominal coverage probability $\psi^{cp} = 0.95$, **Grey horizontal line:** Nominal coverage probability for the lower and the upper limit, if equal tail probabilities are achieved $\psi^l = \psi^u = 0.975$

5.2 Coverage probabilities for the simulation setting inspired by long term carcinogenicity studies

This part of the simulation was inspired by the estimates for the binomial proportion and overdispersion reported by Menssen and Schaarschmidt 2019 for HCD obtained from long term carcinogenicity (LTC) studies run with B6C3F1 mice. In order to assess the coverage probabilities for each of the six methods on a broad range of realistic parameter combinations, the simulation was run for all 96 combinations of $H = 5, 10, 20, 100$, $\pi = 0.01, 0.1, 0.2, 0.3, 0.4, 0.5$, $\phi = 1.001, 1.5, 3, 5$ and a fixed cluster size of $n_h = n^* = 50 \quad \forall \quad h =$

$1, \dots, H$.

Due to the relatively small cluster size, the underlying distribution is heavily discrete and can become heavily right skewed for small proportions and/or high overdispersion. Hence, it is possible that in some settings (especially $\pi = 0.01$) the data contains many zeros. If it happened that a sampled "historical" data set contained only zeros ($y_h = 0 \quad \forall \quad h = 1, \dots, H$), the first observation was set to $y_1 = 0.5$ and the corresponding cluster size was set to $n_1 = 49.5$ following Menssen and Schaarschmidt 2019. This procedure was applied to all frequentist methods (heuristics and prediction intervals) in order to enable the estimation process in this extreme settings, whereas otherwise, the estimates for the binomial proportion and overdispersion would become zero.

Bayesian hierarchical modeling did not lead to convergence regularly enough for reliable results to be reported. In particular, the precision hyperparameter related to overdispersion is very difficult to estimate, which also depends on the prior choice. Therefore, the GLMM is applied here as an alternative.

The heuristical methods (Fig. 3) behaved in a similar fashion than in the MNT-setting: With rising amount of historical control groups, the coverage probability of the range approaches one (Fig. 3A). In the absence of overdispersion, the np-Chart (Fig. 3B) yields coverage probabilities close to the nominal level, but with a rising amount of overdispersion, its coverage probabilities decrease below 0.6.

With a rising amount of historical control groups (at least 20), the coverage probabilities of the HCL computed by the mean ± 2 SD (Fig. 3C) approach the nominal level, if the underlying distribution is relatively symmetrical (low overdispersion and relatively high proportion). With increasing right-skewness of the underlying distribution (increasing overdispersion and decreasing proportion) and /or a low amount of historical control groups ($H < 20$) the HCL computed by the mean ± 2 SD yield coverage probabilities below the nominal level that can decrease to approximately 85 %.

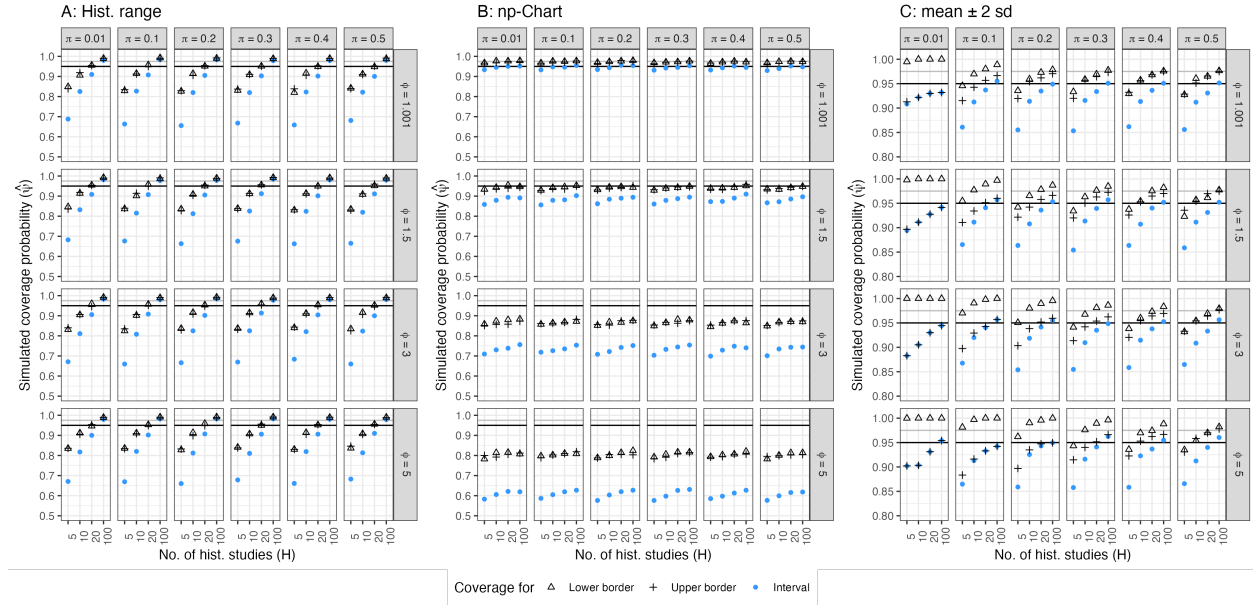


Figure 3: Simulated coverage probabilities of heuristical methods (LTC-setting) **A:** Historical range, **B:** np-chart, **C:** Mean \pm 2 SD, **Black horizontal line:** Nominal coverage probability $\psi^{cp} = 0.95$, **Grey horizontal line:** Nominal coverage probability for the lower and the upper limit, if equal tail probabilities are achieved $\psi^l = \psi^u = 0.975$. Note the different scales of the y-axis of the sub-graphics (0.5-1 for A and B, 0.8-1 for C).

In the practical absence of overdispersion ($\phi = 1.001$), the beta-binomial prediction interval (Fig. 4A) yields coverage probabilities satisfactorily close to the nominal 0.95 (except for $\pi = 0.01$), whereas the prediction intervals that are based on the quasi-binomial assumption (Fig. 4B) or drawn from a Bayesian GLMM (Fig. 4C) tend to remain conservative.

For $\pi \geq 0.2$, moderate overdispersion ($\phi \in [1.5, 3]$) and at least 10 historical control groups ($H \geq 10$) the coverage probabilities of the two frequentist prediction intervals satisfactorily approach the nominal 0.95, whereas the prediction interval obtained from the Bayesian GLMM remains slightly conservative, but may also be practically applicable in this scenario. Contrary, for high overdispersion ($\phi = 5$), the quasi-binomial and the Bayesian prediction interval yield coverage probabilities satisfactorily close to the nominal level (if $\pi \geq 0.2$ and $H \geq 10$). In this setting, the beta-binomial prediction interval yields coverage probabilities below the nominal level for $H = 5$ and remains conservative for $H = 10, 20$, but approaches the nominal level for $H = 100$.

With increasing overdispersion ϕ and decreasing proportions $\pi \leq 0.1$ the amount of zeros and hence the right skeweness of the underlying distribution increases. This means that the lower borders of all three prediction intervals tend to cover more future observations than desired. This is the reason why all three prediction intervals practically yield 97.5 % upper prediction borders for $\pi = 0.01$ and the conservativeness of the lower borders increases for $\pi = 0.1$ with an increase of ϕ . This is not a misbehavior of the methodologies, but rather reflects a core feature of the underlying distribution.

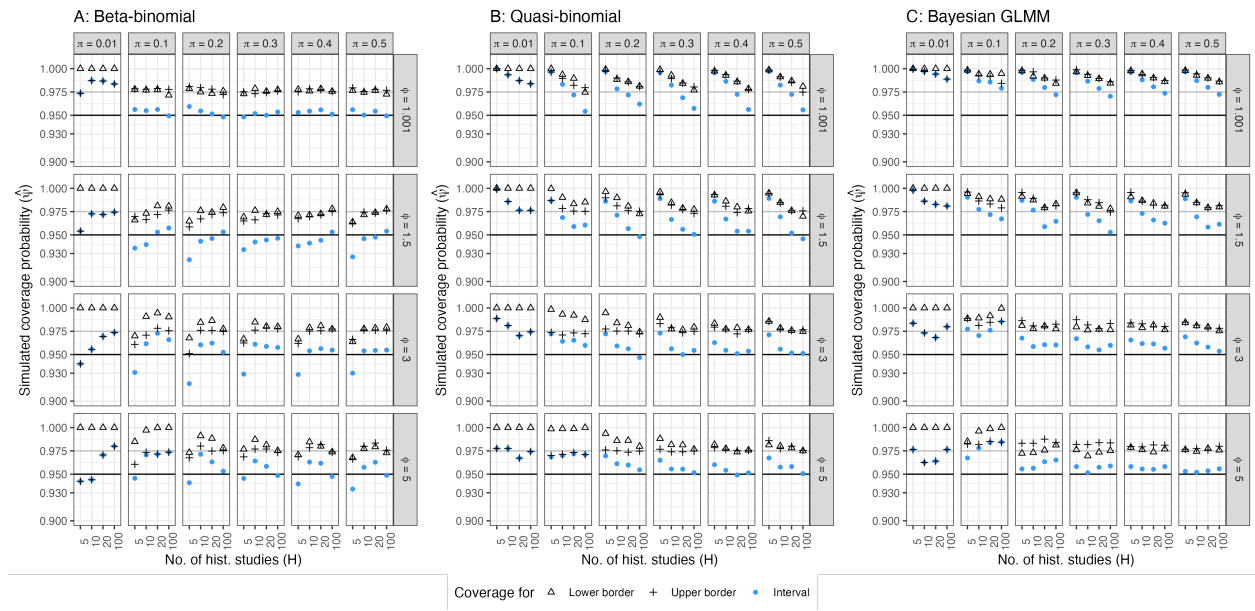


Figure 4: Simulated coverage probabilities of prediction intervals (LTC-setting) **A:** Calibrated beta-binomial prediction interval, **B:** Calibrated quasi-binomial prediction interval, **C:** Prediction interval obtained from a Bayesian GLMM, **Black horizontal line:** Nominal coverage probability $\psi^{cp} = 0.95$, **Grey horizontal line:** Nominal coverage probability for the lower and the upper limit, if equal tail probabilities are achieved $\psi^l = \psi^u = 0.975$.

6 Application of control limits

The calculation of HCL based on real life data is demonstrated using HCD about the mortality of male B6C3F1-mice in long-term carcinogenicity studies ($n_h = n^* = 50$). The

data set was provided by Menssen and Schaarschmidt 2019 and contains negative controls from 10 different studies run between 2003 and 2011 on behalf of the NTP. It is available via the `predint` R package (Menssen 2024) under the name `mortality_HCD`.

The estimate for the binomial proportion is $\hat{\pi} = 0.276$ and slight overdispersion of $\hat{\phi} = 1.31$ appears to be present in the data (estimated with `stats::glm()`). The R code for the computation of the different HCL depicted in table 1 is available from GitHub (see link provided in section 3.4).

Table 1: Control limits (CL) for the mortality of male B6C3F1-mice obtained in negative controls of long term carcinogenicity studies at the National Toxicology Program.

Method	Lower CL	Upper CL	Interval width
Hist. range	10 (10)	21 (21)	11 (11)
np-chart	7.47 (8)	20.12 (20)	12.65 (12)
Mean \pm 2 SD	6.57 (7)	21.03 (21)	14.46 (14)
Beta-binomial ¹	6.33 (7)	22.24 (22)	15.91 (15)
Quasi-binomial (QP) ²	5.77 (6)	22.71 (22)	16.94 (16)
Bayesian hierarchical ³	7 (7)	21.025 (21)	14.025 (14)
Bayesian GLMM	6 (6)	23 (23)	17 (17)

Numbers in brackets: Lowest and highest number of events covered by the interval.

1: Estimates $\hat{\pi} = 0.276$ and $\hat{\rho} = 0.00621$ were obtained following Lui et al. 2000 (see computational details)

2: Estimates $\hat{\pi} = 0.276$ and $\hat{\phi} = 1.31$ were obtained based on `stats::glm` (see computational details)

3: A weakly informative prior $\kappa \sim \text{Ga}(2, 5 \cdot 10^{-3})$ was used.

The historical range yields the highest lower limit and the lowest upper limit and hence, the shortest control interval of all seven methods. Of the six methods that are aimed to cover a future observation with a probability of 0.95, the np-chart yields the shortest interval, because it does not account for the presence of overdispersion.

Practically, the mean \pm 2 SD and the prediction interval obtained from Bayesian hierarchical modeling yield the same limits [7, 21]. Both calibrated prediction intervals practically yield upper limits of 22 but the lower limit of the quasi-binomial prediction interval is slightly lower than the beta-binomial one (6 vs. 7). With limits [6, 23], the prediction interval drawn from a Bayesian GLMM is the widest one and hence is in line with the simulation results that

revealed a slightly conservative behaviour for a comparable LTC setting of $\phi = 1.5$, $H = 10$ and $\pi = 0.2$ (see Fig. 4C).

Note that, contrary to the description of the Bayesian hierarchical model given in section 3.4 (which basically aims at the MNT-inspired setting) a weakly informative prior $\kappa \sim \text{Ga}(2, 5 \cdot 10^{-3})$ was used for the precision hyperparameter κ . This adaption was necessary to reach convergence of the model.

7 Discussion

The validation of a concurrent control group based on prediction intervals is recommended by several authors (Menssen 2023, Kluxen et al. 2021) and since shortly, seems to be preferred by the European Food Safety Agency (EFSA 2024) over other (heuristical) methods. Nevertheless, since literature for the calculation of prediction intervals for clustered dichotomous data is relatively scarce, the practical application of HCL tends to rely on several heuristics, such as the application of the mean ± 2 SD (Rotolo et al. 2021, Prato et al. 2023, de Kort et al. 2020, Kluxen et al. 2021) or limits from Sheward control charts (Lovell et al. 2018, Dertinger et al. 2023). Our simulations have shown that these heuristical methods do not control the statistical error to a satisfactory level and hence, these methods can not be recommended for the practical validation of a current control group.

Valverde-Garcia et al. 2018 report HCD for avian reproduction and calculated prediction intervals for several dichotomous endpoints such as the number of viable vs. nonviable hatchlings. Anyhow, the applied prediction intervals depend on the assumption of univariate normality and hence do not match with the dichotomy of the assessed endpoints.

Several prediction intervals are available from the literature that are based on the assumption of independent binomial distributed observations (Meeker et al. 2017), but ignore the clustered structure of the HCD (and hence the possibility for between-study overdispersion). Menssen and Schaarschmidt 2019 showed, that these intervals fail to approach the nominal coverage probability in the presence of overdispersion.

The magnitude of overdispersion reflects the between-study variation which is commonly

present in toxicological HCD and hence, can be found in several published HC data sets in the literature (Tarone 1982a, Tarone 1982b, Levy et al. 2019, Menssen et al. 2024, Carlus et al 2013, Dertinger et al. 2023, Tug et al. 2024, see supplementary materials section 4). Therefore prediction intervals that are based on the simple binomial assumption can not be recommended for their application to HCD with a toxicological background. The need for methodology that account for between-study overdispersion was addressed by the proposed prediction intervals. All four methods explicitly account for the clustered structure of toxicological HCD and hence also for the possible presence of overdispersion.

Both of the calibrated prediction intervals are improved versions of the quasi-binomial prediction interval of Menssen and Schaarschmidt 2019 which rely on a bootstrap procedure that adapts the formerly symmetrical prediction interval to possible skeweness of the underlying distribution. Note, that this bootstrap calibration procedure has already been applied successfully for the calculation of prediction intervals drawn from random effects models (Menssen and Schaarschmidt 2022) or for overdispersed count data (Menssen et al. 2024). This means that, as long as one is able to bootstrap new observations from a model and the prediction standard error $\widehat{se}(\hat{y}^* - Y^*) = \sqrt{\widehat{var}(\hat{y}^*) + \widehat{var}(Y^*)}$ can be formulated, the presented bootstrap calibration procedure provides a standardized framework for the calculation of prediction intervals for various distributional assumptions and/or models. An implementation of the bisection used in step 8 and 9 of the bootstrap calibration is provided via the function `bisection()` of the `predint` R package.

The prediction intervals drawn from Bayesian hierarchical models yield coverage probabilities that in the MNT-setting mainly remain below the nominal level (if overdispersion is present), but the model did not converge to most of the simulated data sets that mimic HCD from carcinogenicity studies (mainly if many zeros were present in the data). It is noteworthy, that in the Monte-Carlo simulations, Bayesian hierarchical models were fit, always using the same prior $\kappa \sim \text{Ga}(2, 5 \cdot 10^{-5})$ regardless of the simulation setting. But, from the application to the real life example it is obvious, that this type of model needs a case to case adaption of the prior distribution to provide a reasonable domain for the hyperparameter κ (which depends on the amount of overdispersion). This might, at least partly, explain the liberality of this

method. Unfortunately, the necessity for a case by case adaption of the prior distribution is far beyond the scope of most practitioners who are in charge of the reporting of HCD (mainly toxicologists that are barely trained in statistics). Hence this necessity might be a drawback for practical application.

Contrary to the Bayesian hierarchical models, the Bayesian GLMM did not have convergence problems in the LTC-setting. But, the applied GLMM mainly yield prediction intervals with coverage probabilities above the nominal level (except for a higher amount of overdispersion). This is, because such models a priori assume overdispersion (or, equivalently, additional non-zero between-study variance) to be present, and estimate the respective parameters, even if they are actually not part of the data-generating process.

An alternative to a fully Bayesian approach might be the application of an empirical Bayes procedure in which the hyperparameter's domain is pre-estimated from the HCD, similar to the approaches of Tarone 1982a who incorporated HCD in a trend test or Kitsche et al. 2012 who exploit HCD to be accounted for in a Dunnett-type mean comparison. Anyhow, to the authors knowledge, an empirical Bayes procedure for the calculation of prediction intervals for overdispersed binomial data does not exist and might be a subject for future research.

It is noteworthy, that the coverage probability of the calibrated intervals is mainly effected by the amount of available historical information and that in most of the cases the amount of overdispersion or the magnitude of the binomial proportion is of minor importance. This means, that for a high cluster size (as in the MNT-setting) both calibrated prediction intervals yield coverage probabilities satisfactorily close to the nominal level even for only five historical control groups. Contrary, for smaller cluster sizes (as in the LTC-setting) the number of historical control groups has to be slightly higher (say 10) to enable coverage probabilities close enough to the nominal level. Furthermore, note that with decreasing cluster size, the discreteness of the underlying distribution rises and hence, the nominal 0.95 coverage probability can not completely be achieved in all of the possible cases (Agresti 1998).

Since the bootstrap calibration procedure presented above has already been applied to enable the calculation of prediction intervals drawn from linear random effects models (Menssen and Schaarschmidt 2022) or in order to predict overdispersed count data (Menssen et al. 2024),

it can be seen as a general and flexible tool for the calculation of prediction intervals. Hence, for the future it is planned to exploit its potential to enable the calculation for a broader range of models / distributions. Furthermore it is possible to extend the algorithm to enable the calculation of simultaneous prediction intervals, which also will be the subject of future research.

Another relevant application is the evaluation of HCD with individual (non-aggregated) values reported (e.g., for six wells in one historical MNT-experiment), where extra-Binomial variability is also possible within one experiment. Here, GLMMs (both frequentist and Bayesian) as well as hierarchical models can be very helpful. Jeske and Young 2013 provided a bootstrap based procedure for the calculation of prediction intervals based on one-way GLMM, but to the authors knowledge, a general solution for the calculation of prediction intervals drawn from GLMM is not yet available. Hence, also this topic remains as an open issue.

8 Conclusions

If overdispersion is present in the data (and its magnitude is tolerable):

- Commonly applied heuristics (e.g. hist. range, np-charts or mean \pm 2 SD) do not satisfactorily control the statistical error and hence, should not be applied for the calculation of HCL.
- Symmetrical HCL do not account for possible right- (or left-) skeweness of the data and hence do not ensure for equal tail probabilities.
- In most of the cases, the bootstrap calibrated prediction intervals yield coverage probabilities closest to the nominal level and hence, outperform all other methods reviewed in this manuscript.
- In most of the cases, the Bayesian prediction intervals do not yield coverage probabilities close enough to the nominal level (Bayesian hierarchical prediction intervals remain liberal, prediction intervals drawn from Bayesian GLMMP tend to behave conservatively).

- With an increasing amount of overdispersion and decreasing binomial proportion, the amount of zeros in the data increases. If the amount of zeros in the data is high enough, the lower border will always cover the future observation and consequently prediction intervals (Bayesian or frequentist) practically yield 97.5 % upper prediction limits. This behavior is not a drawback of the methodology, but rather reflects one of the core features of overdispersed binomial data.
- Software for the calculation of bootstrap calibrated prediction intervals is publicly available via the R package `predint`.

9 References

Bonapersona, V., Hoijtink, H., RELACS Consortium Abbinck M. 4 Baram TZ 5 6 Bolton JL 5 Bordes J. 7 Knop J. 1 Korosi A. 4 Krugers HJ 4 Li JT 8 9 Naninck EFG 4 Reemst K. 4 Ruigrok SR 4 Schmidt MV 7 Umeoka EHL 4 10 Walker CD 11 Wang XD 12 Yam KY 4, Sarabdjitsingh, R. A., Joëls, M. (2021). Increasing the statistical power of animal experiments with historical control data. *Nature neuroscience*, 24(4), 470-477.

Carlus, M., Elies, L., Fouque, M. C., Maliver, P., Schorsch, F. (2013). Historical control data of neoplastic lesions in the Wistar Hannover Rat among eight 2-year carcinogenicity studies. *Experimental and Toxicologic Pathology*, 65(3), 243-253.

de Kort, M., Weber, K., Wimmer, B., Wilutzky, K., Neuenhahn, P., Allingham, P., Leoni, A. L. (2020). Historical control data for hematology parameters obtained from toxicity studies performed on different Wistar rat strains: Acceptable value ranges, definition of severity degrees, and vehicle effects. *Toxicology Research and Application*, 4, 2397847320931484.

Demétrio, C. G., Hinde, J., Moral, R. A. (2014). Models for overdispersed data in entomology. *Ecological modelling applied to entomology*, 219-259.

Dertinger, S. D., Li, D., Beevers, C., Douglas, G. R., Heflich, R. H., Lovell, D. P., Roberts,

D.J., Smith, R., Uno, Y., Williams, A., Witt, K.L., Zeller A., Zhou, C. (2023). Assessing the quality and making appropriate use of historical negative control data: A report of the International Workshop on Genotoxicity Testing (IWGT). *Environmental and Molecular Mutagenesis*.

EFSA (2024): Draft Scientific Opinion on the use and reporting of historical control data for regulatory studies. Public Consultation PC-0856. <https://connect.efsa.europa.eu/RM/s/consultations/publicconsultation2/a01Tk000000Cvs9/pc0856>

Fenech, M. (2000). The in vitro micronucleus technique. *Mutation Research/Fundamental and Molecular Mechanisms of Mutagenesis*, 455(1-2), 81-95.

Fong, Y., Rue, H., Wakefield, J. (2010). Bayesian inference for generalized linear mixed models. *Biostatistics*, 11(3), 397-412.

Francq, B. G., Lin, D., Hoyer, W. (2019). Confidence, prediction, and tolerance in linear mixed models. *Statistics in medicine*, 38(30), 5603-5622.

Gabry, J., Goodrich, B., Ali, I., Brilleman, S. (2024). Bayesian applied regression modeling via Stan. R Package rstanarm, version 2.32.1

Greim, H., Gelbke, H. P., Reuter, U., Thielmann, H. W., Edler, L. (2003). Evaluation of historical control data in carcinogenicity studies. *Human & experimental toxicology*, 22(10), 541-549.

Gurjanov, A., Kreuchwig, A., Steger-Hartmann, T., Vaas, L. A. I. (2023). Hurdles and signposts on the road to virtual control groups—a case study illustrating the influence of anesthesia protocols on electrolyte levels in rats. *Frontiers in Pharmacology*, 14, 1142534.

Gurjanov, A., Vieira-Vieira, C., Vienenkoetter, J., Vaas, L. A., Steger-Hartmann, T. (2024a).

Replacing concurrent controls with virtual control groups in rat toxicity studies. *Regulatory Toxicology and Pharmacology*, 148, 105592.

Gurjanov, A., Vaas, L. A., Steger-Hartmann, T. (2024). The road to virtual control groups and the importance of proper body-weight selection. *ALTEX-Alternatives to animal experimentation*.

Hamada, M., Johnson, V., Moore, L. M., Wendelberger, J. (2004). Bayesian prediction intervals and their relationship to tolerance intervals. *Technometrics*, 46(4), 452-459.

Hoffman, D. (2003). Negative binomial control limits for count data with extra-Poisson variation. *Pharmaceutical Statistics: The Journal of Applied Statistics in the Pharmaceutical Industry*, 2(2), 127-132.

Howley, P. P., Gibberd, R. (2003). Using hierarchical models to analyse clinical indicators: a comparison of the gamma-Poisson and beta-binomial models. *International Journal for Quality in Health Care*, 15(4), 319-329.

Jeske, D. R., Yang, C. H. (2013). Approximate Prediction Intervals for Generalized Linear Mixed Models Having a Single Random Factor. *Statistics Research Letters*, 2(4), 85-95.

Kitsche, A., Hothorn, L. A., Schaarschmidt, F. (2012). The use of historical controls in estimating simultaneous confidence intervals for comparisons against a concurrent control. *Computational Statistics & Data Analysis*, 56(12), 3865-3875.

Kluxen, F. M., Weber, K., Strupp, C., Jensen, S. M., Hothorn, L. A., Garcin, J. C., Hofmann, T. (2021). Using historical control data in bioassays for regulatory toxicology. *Regulatory Toxicology and Pharmacology*, 125, 105024.

McCullagh P, Nelder J.A. (1989): *Generalized Linear Models*. 2nd Edition, Chapman and Hall, London.

Meeker, W. Q., Hahn, G. J., Escobar, L. A. (2017). Statistical intervals: a guide for practitioners and researchers. John Wiley & Sons.

Montgomery, D. C. (2019). Introduction to statistical quality control. John Wiley & Sons.

Nelson, W. (1982). Applied Life Data Analysis. New York, NY: John Wiley & Sons.

Lovell, D. P., Fellows, M., Marchetti, F., Christiansen, J., Elhajouji, A., Hashimoto, K., Kasamotog, S., Lih, Y., Masayasui, O., Moorej, M.M., Schulerk, M., Smithl, R., Stankowski Jr.m,L.F., Tanakag, J., Tanirn, J.Y., Thybaudo, V., Van Goethemp F., Whitwell, J. (2018). Analysis of negative historical control group data from the in vitro micronucleus assay using TK6 cells. *Mutation Research/Genetic Toxicology and Environmental Mutagenesis*, 825, 40-50.

Lui, K. J., Mayer, J. A., Eckhardt, L. (2000). Confidence intervals for the risk ratio under cluster sampling based on the beta-binomial model. *Statistics in medicine*, 19(21), 2933-2942.

Levy, D. D., Zeiger, E., Escobar, P. A., Hakura, A., Bas-Jan, M., Kato, M., Moore, M.M., Sugiyama, K. I. (2019). Recommended criteria for the evaluation of bacterial mutagenicity data (Ames test). *Mutation Research/Genetic Toxicology and Environmental Mutagenesis*, 848, 403074.

McCullagh P, Nelder J.A. (1989): Generalized Linear Models. 2nd Edition, Chapman and Hall, London.

Meeker, W. Q., Hahn, G. J., Escobar, L. A. (2017). Statistical intervals: a guide for practitioners and researchers. John Wiley & Sons.

Menssen, M., Schaarschmidt, F. (2019). Prediction intervals for overdispersed binomial data

with application to historical controls. *Statistics in Medicine*, 38(14), 2652-2663.

Menssen, M., Schaarschmidt, F. (2022). Prediction intervals for all of M future observations based on linear random effects models. *Statistica Neerlandica*, 76(3), 283-308.

Menssen, M. (2023). The calculation of historical control limits in toxicology: Do's, don'ts and open issues from a statistical perspective. *Mutation Research/Genetic Toxicology and Environmental Mutagenesis*, 503695.

Menssen M (2024). *predint: Prediction Intervals*. R package version 2.2.1

Menssen, M., Dammann, M., Fneish, F., Ellenberger, D., Schaarschmid, F. (2024). Prediction intervals for overdispersed Poisson data and their application in medical and pre-clinical quality control. (under review) arXiv preprint arXiv:2404.05282.

Montgomery, D. C. (2019). *Introduction to statistical quality control*. John Wiley & Sons.

Nelson, W. (1982). *Applied Life Data Analysis*. New York, NY: John Wiley & Sons.

NTP (2024): NTP Historical Controls Data Base. <https://ntp.niehs.nih.gov/data/controls>

OECD 471: Bacterial Reverse Mutation Test, OECD Guidelines for the Testing of Chemicals, Section 4, OECD Publishing, Paris.

OECD 473: In Vitro Mammalian Chromosomal Aberration Test, OECD Guidelines for the Testing of Chemicals, Section 4, OECD Publishing, Paris

OECD 487: In Vitro Mammalian Cell Micronucleus Test, OECD Guidelines for the Testing of Chemicals, Section 4, OECD Publishing, Paris.

OECD 489: In Vivo Mammalian Alkaline Comet Assay, OECD Guidelines for the Testing of Chemicals, Section 4, OECD Publishing, Paris.

OECD 490: In Vitro Mammalian Cell Gene Mutation Tests Using the Thymidine Kinase Gene, OECD Guidelines for the Testing of Chemicals, Section 4, OECD Publishing, Paris.

Prato, E., Biandolino, F., Parlapiano, I., Grattagliano, A., Rotolo, F., Buttino, I. (2023). Historical control data of ecotoxicological test with the copepod *Tigriopus fulvus*. Chemistry and Ecology, 39(8), 881-893.

Rotolo, F., Vitiello, V., Pellegrini, D., Carotenuto, Y., Buttino, I. (2021). Historical control data in ecotoxicology: Eight years of tests with the copepod *Acartia tonsa*. Environmental Pollution, 284, 117468.

Ryan, L. (1993). Using historical controls in the analysis of developmental toxicity data. Biometrics, 1126-1135.

Spiliotopoulos, D., Koelbert, C., Audebert, M., Barisch, I., Bellet, D., Constans, M., Czich, A., Finot, F., Gervais, V., Khoury, L., Kirchnawy, C., Kitamoto, S., Le Tesson, A., Malesic, L., Matsuyama, R., Mayrhofer, E., Mouche, I., Preikschat, B., Prielinger, L., Rainer, B., Roblin, C., Wäse, K. (2024). Assessment of the performance of the Ames MPFTM assay: A multicenter collaborative study with six coded chemicals. Mutation Research/Genetic Toxicology and Environmental Mutagenesis, 893, 503718.

Stan Development Team. (2024) RStan: the R interface to Stan. R package version 2.32.6.

Stan Development Team (2024). Stan functions reference. version 2.35.27

Tarone, R. E. (1982a). The use of historical control information in testing for a trend in

proportions. *Biometrics*, 215-220.

Tarone, R. E. (1982b). The use of historical control information in testing for a trend in Poisson means. *Biometrics*, 457-462.

Tug, T., Duda, J. C., Menssen, M., Bruce, S. W., Bringezu, F., Dammann, M., Frotschl, R., Harm, V., Ickstadt, K., Igl, B-W., Jarzombek, M., Kellner, R., Lott, J., Pfuhler, S., Plappert-Helbig, U., Rahnenfuhrer, J., Schulz, M., Vaas, L., Vasquez, M., Ziegler, V., Ziemann, C. (2024). In vivo alkaline comet assay: Statistical considerations on historical negative and positive control data. *Regulatory Toxicology and Pharmacology*, 148, 105583.

Valverde-Garcia, P., Springer, T., Kramer, V., Foudoulakis, M., Wheeler, J. R. (2018). An avian reproduction study historical control database: a tool for data interpretation. *Regulatory Toxicology and Pharmacology*, 92, 295-302.

Vandenberg, L. N., Prins, G. S., Patisaul, H. B., Zoeller, R. T. (2020). The use and misuse of historical controls in regulatory toxicology: lessons from the CLARITY-BPA study. *Endocrinology*, 161(5), b0z014.